Can a Hydroxide Ligand Trigger a Change in the Coordination Number of Magnesium Ions in Biological Systems?†

Stefan Kluge and Jennie Weston*

Institut für Organische Chemie und Makromolekulare Chemie der Friedrich-Schiller-Universität, Humboldtstrasse 10, D-07743 Jena, Germany

Received December 6, 2004; Revised Manuscript Received January 25, 2005

ABSTRACT: Density functional (B3LYP) calculations indicate that a hydroxide ligand is capable of triggering a reduction in the coordination number of Mg^{2+} ions from 6 to 5. Since this could be quite relevant in the mode of action of magnesium-containing enzymes (especially hydrolases in which a metal-bound hydroxide species is believed to play a crucial role), we have performed a systematic deprotonation study of biologically relevant magnesium complexes. We explicitly calculated the preferred coordination number of $[MgL^1_xL^2_yL^3_z]^{2-n}$ species at the B3LYP/aug-cc-pVTZ level of theory. L^1, L^2, and L^3 represent combinations of water, hydroxide, carboxylate (models Glu and Asp), ammonia ligands (models Lys and His residues), and fluoride ions. As expected, Mg^{2+} exclusively prefers an octahedral coordination geometry with H_2O, HCO_2^-, or NH_3. Surprisingly, *one hydroxide ligand triggers a change to a trigonal bipyramidal geometry*. The isoelectronic fluoride ion behaves similarly. When two OH^- are present, a tetrahedral coordination geometry is preferred. We postulate that a hydroxide (in addition to its role as an active nucleophile) could be employed by magnesium-containing enzymes to trigger a differential coordination behavior.

Magnesium is an essential element for numerous biochemical functions in cell processes (*1*), although exactly why this is so is still not fully understood. Clearly, its relatively large intracellular concentration as compared to other divalent metal ions plays an important role (*2*). In addition, two fundamentally different biological binding mechanisms (inner sphere and outer sphere) are observed for magnesium (*1*, *3*, *4*). Nucleic acids bind to Mg^{2+} ions via a water molecule in its second coordination sphere (indirect mechanism) whereas enzymes prefer to bind Mg^{2+} directly to organic ligands originating from the protein backbone in the immediate vicinity of the active site (*5*).

In aqueous solutions, numerous experimental (*6*, *7*) and theoretical studies (*7*, *8*) on hydrated Mg^{2+} all agree that the first coordination shell of the metal ion is completed with six water molecules in an octahedral arrangement. In accord with this, there are numerous solid-state structures of hexaaquomagnesium salts deposited in X-ray structural databanks worldwide (*9*). The direct cation−water interactions in the first solvent shell of $Mg[H_2O]_6^{2+}$ are mainly electrostatic in nature although some charge is transferred from oxygen to the magnesium ion (*10g*). If there are more than six waters, they arrange themselves in the second coordination sphere of the ion (*6a*). It is still not known exactly how many water molecules can be placed in the second coordination sphere although the current estimate indicates 12 (*7a*). Removal of a water from the outer sphere of $[Mg(H_2O)_6]^{2+}$ costs approximately 5−12 kcal/mol (*6a,c*) whereas removal of an inner sphere ligand is much more difficult (20−80 kcal/mol) and strongly depends on the extent of hydration (*8*).

Several theoretical competitive binding studies of water vs ligands of biological interest (HCO_2^-, HCO_2H; formamide and methanol) have been performed for Mg^{2+} ions (*10*). It could be shown that the dielectric properties of the solvent play a critical role in determining the mode of magnesium binding. In regions where a low ($\epsilon \leq 4$) dielectric medium is present (protein cavities) a hexaaquomagnesium ion has a high affinity for negatively charged acidic residues (carboxylate rests) (*10b,c*). The exchange of water for formate ions is thermodynamically favored until an upper limit of three is reached (*10b,c*). As the dielectric constant increases and approaches that of bulk water, further exchange becomes increasingly disfavored (*10b,c*). All of these computational studies have *assumed* that magnesium is hexacoordinated both in solution and in the protein cavity and water molecules were added as necessary to complete the first coordination sphere.

In the context of organometallic chemistry, it is frequently observed that Mg^{2+} complexes exhibit a coordination number of 4 (*11*), which has been interpreted as a result of steric interactions associated with bulky ligands used to stabilize the ion (*12*). It is quite clear that a variable coordination number (4−6) for Mg^{2+} is fundamentally possible, although hexacoordination is almost invariably observed in aqueous solutions. Electrospray ionization experiments in the gas phase have recently shown that isolated $[Mg(H_2O)_6]^{2+}$ ions exist in two different isomeric forms (*13*). DFT calculations

† Financial support by Land Thüringen, Germany, and by the Deutsche Forschungsgemeinschaft (Sonderforschungsbereich 436, Jena, Germany) is gratefully acknowledged.

* To whom correspondence should be addressed. E-mail: Jennie.Weston@uni-jena.de. Telephone: +41 (0) 3641-9-48224. Fax: +41 (0) 3641-9-48211.

10.1021/bi047454j CCC: $30.25
Published on Web 03/01/2005

postulate these to have hexacoordinated $[Mg(H_2O)_6]^{2+}$ and pentacoordinated $[Mg(H_2O)_6]^{2+}\cdot H_2O$ structures (*8c*, *10d*, *13*).

Quite a few magnesium-containing enzymes catalyze the hydrolytic cleavage of a phosphate ester (nucleases, polymerases, phosphatases, etc.), and their mode of action is often postulated to involve the deprotonation of a metal ion-bound water molecule to yield a metallohydroxide which then acts as a nucleophile to attack a substrate (*14*). However, far fewer computational and/or experimental studies of magnesium−hydroxide bonding have been reported in the literature than hydration studies with most having concentrated on small metal−ligand adducts $[M(OH)_n, n = 1-3]$ in the gas phase (*15*, *16*). Deprotonation of a water molecule in hydrated $[Mg(H_2O)_6]^{2+}$ has, to our knowledge, only been very briefly mentioned (*10g*, *16*).

Magnesium ions are quite labile, and this coupled with their spectroscopic silence makes direct experimental observations of the binding mode of Mg^{2+} in enzymes or biomimetic complexes extremely difficult. In the few cases where single crystals of magnesium-containing enzymes have been obtained, the extremely low electron density of Mg^{2+} has usually been quite problematical in satisfactorily resolving the active site structure.

In the course of developing a computational model for the active site of inositol monophosphatase (*17*), we have discovered that, under certain circumstances, the preferred coordination number of Mg^{2+} can be lowered from 6 to 5 or even 4. We have therefore performed an extensive density functional study of the influence of the ligand sphere on the coordination number of magnesium species in the presence of water and biologically relevant ligands.

COMPUTATIONAL DETAILS

The calculations reported in this paper were performed with the gradient-corrected, partially correlated B3LYP (*18*) density functional using either the Gaussian98 (*19*) or the Gaussian03 (*20*) program package. H, C, N, O, and F were described with the very large correlation consistent aug-cc-pVTZ basis set (*21*). Dunning's cc-pVTZ basis was employed for the central Mg^{2+} ion (*22*). The (quite a bit smaller) 6-31+G* basis set has been shown to systematically slightly overestimate ΔG_{rel} values for hydrated Mg^{2+} species at the B3LYP level of theory (*10e*). However, the errors did not exceed 1 kcal/mol. Basis set superposition errors (BSSE) were reported to be rather small (0.5 → 1.1 kcal/mol), and correcting the theoretical ΔG_{rel} values for BSSE *increased* the systematic overestimation as compared to experimental values (*10e*). It has therefore been recommended to omit BSSE corrections for the B3LYP method (*10e*). In accord with these findings, our ΔG_{rel} values [which were calculated with the very much larger aug-cc-pVTZ basis (cc-pVTZ on Mg^{2+})] do not contain a BSSE correction. For some of the mixed ligand species, we employed the smaller lanl2dz basis, which we found to deliver qualitatively the same structural results as the larger aug-cc-pVTZ basis. Better energies were then obtained for the lanl2dz geometries by single point calculations at the B3LYP/aug-cc-pVTZ level. Default convergence criteria were used for all calculations. No symmetry was employed in any of the calculations, and coordination geometries other than 6 were explicitly explored. The stationary points found were characterized as minima by calculating their vibrational frequencies. When trying to differentiate between a transition structure with a low-lying frequency and an energetical minimum (structure **1a**, for example), we reoptimized using Grid=ultrafine. All relative stabilities reported are gas phase Gibb's free energies that contain standard thermochemical and vibrational corrections. Solvation effects (both specific and bulk) are currently being investigated in detail and will be discussed in a forthcoming paper. Natural bond orbital [NBO (*23*)] analyses of the magnesium complexes were carried out at the B3LYP/aug-cc-pVTZ level of theory using NBO version 5.0 as patched into Gaussian98 (*24*).

RESULTS AND DISCUSSION

Hydroxide Ligands. Removal of a proton from a water molecule in $[Mg(OH_2)_6]^{2+}$ and reoptimization at the HF/6-31G* level of theory have been reported to yield a hexacoordinated complex, **1a**, in which the hydroxide is stabilized via hydrogen bonds to two of the water molecules (Figure 1) (*10e*). We were therefore quite surprised when our own investigations at the higher B3LYP/aug-cc-pVTZ level failed to reproduce this structure but led instead to several trigonal bipyramidal structures in which the coordination number of magnesium had been reduced to 5. One of the water molecules previously coordinated to magnesium had spontaneously migrated to the second solvation sphere. The most stable of these conformers (**1b**) is illustrated in Figure 1. After expending some effort, we finally succeeded in locating the hexacoordinated stationary point **1a** only to find that it is a transition structure (with a low-lying negative frequency) for the migration of an equatorial water into the second coordination sphere and lies 7.9 kcal/mol higher than **1b** on the B3LYP hypersurface.

Removing a hydrogen from a second water molecule in **1b** and reoptimization starting from a pentacoordinate geometry continued this trend. A second water molecule spontaneously left the first coordination sphere, and several tetrahedral complexes resulted with **1c** being the most stable minimum. Complexes **1d** (three OH^-) and **1e** (four OH^-) also prefer a tetrahedral coordination. Our calculations indicate that the magnesium ion is not capable of accommodating more than four negative charges in the gas phase since further deprotonations of **1e** and reoptimization lead to an isolated $[Mg(OH)_4]^{2-}$ species and either a $H_3O_2^-$ ion or two isolated OH^- ions.

These changes in the coordination geometry of magnesium upon deprotonation were found to be independent of the starting geometry. Starting from octahedral $[Mg(H_2O)_6]^{2+}$ and removing all protons at once instead of successive deprotonation yielded the same results. The water molecule/molecules that spontaneously migrate always assume a position in the second coordination sphere where they can help to stabilize the hydroxide ligand(s) via direct hydrogen bonding. We then verified that these unusual coordination numbers (5 and 4) are intrinsically stable by removing all second sphere waters in **1b**−**e**. This is indeed the case for **1b′** (pentacoordinate) and **1c′**/**1e′** (tetrahedral), all three of which are stable minima (not illustrated). Without the stabilizing hydrogen bonds originating from specific solvation in the second coordination sphere, complex **1d′** is instable. The water molecule in $[Mg(OH)_3(OH_2)]^-$ migrates

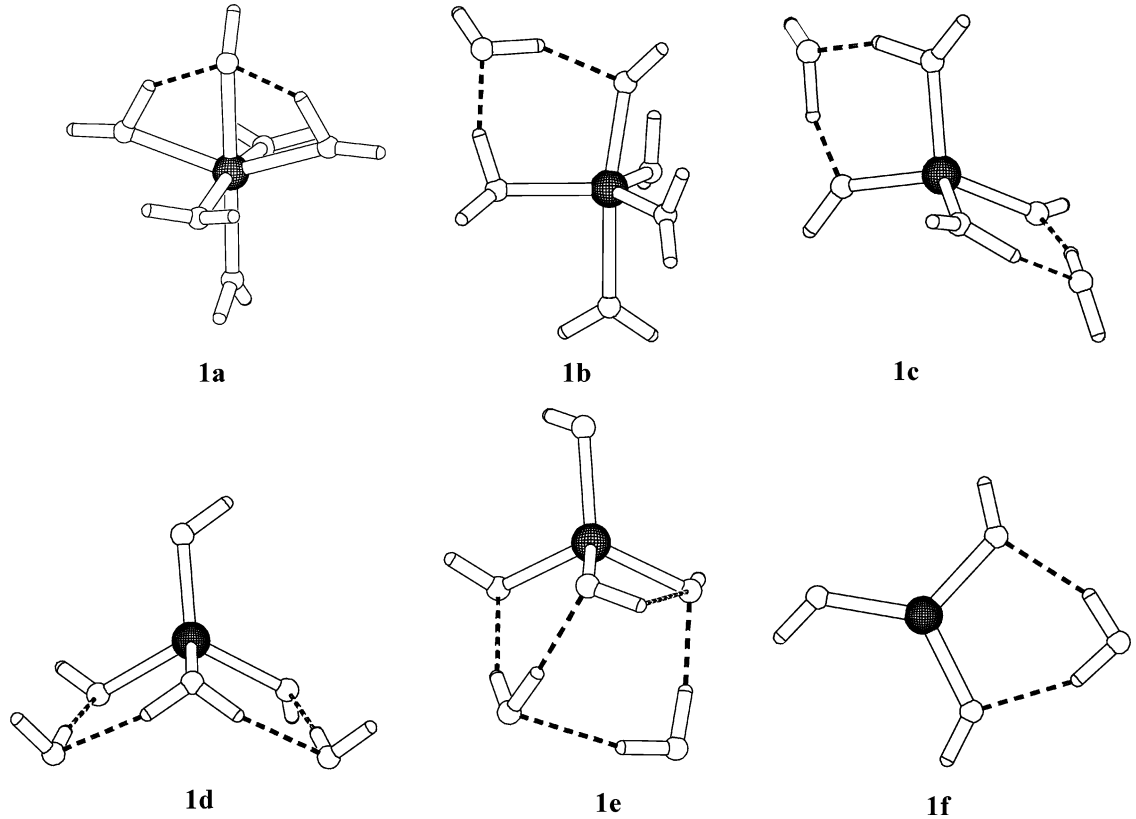

FIGURE 1: Ball and stick diagrams of the most stable conformation of $[Mg(OH)_n(OH_2)_{6-n}]^{2-n}$ ions ($n = 1 \rightarrow 4$). Structure **1a** is a transition structure for the migration of an equatorial water into the second coordination sphere. Calculated at the B3LYP/aug-cc-pVTZ level of theory.

Table 1: Thermodynamical Parameters (kcal/mol) for Deprotonation Reactions of $[Mg(H_2O)_6]^{2+}$ Ions[a]

n	ΔG	ΔH	$T\Delta S$
	$[Mg(H_2O)_6]^{2+} + nH_2O \rightarrow$ $[Mg(OH)_n(H_2O)_{6-n}]^{2-n} + nH_3O^+$		
1[b]	−4.1	−3.9	0.6
2[b]	65.7	64.7	−0.9
3[b]	236.5	235.8	−0.6
4[b]	499.9	500.1	0.2
	$[Mg(H_2O)_6]^{2+} + nH_2O \rightarrow$ $[Mg(OH)_n(H_2O)_{6-n-x}]^{2-n} + nH_3O^+ + xH_2O$		
1[c]	0.8	12.2	10.5
2[c]	76.9	97.0	18.4
3[c]	250.1	280.8	28.1
4[c]	526.4	547.5	19.3

[a] Calculated at the B3LYP/aug-cc-pVTZ level of theory. [b] A total of six ligands are present; Figure 1 shows how many waters are located in the second coordination sphere. [c] In this case, all second sphere waters shown in Figure 1 have been treated as separate entities.

to the second coordination sphere and a planar "ate" complex, **1f** (illustrated in Figure 1), results.

Calculated thermodynamic equilibrium positions for two different deprotonation reactions can be found in Table 1. In the first reaction, all six ligands are explicitly included and were allowed to arrange themselves spontaneously (species **1b**−**e** in Figure 1):

$$[Mg(H_2O)_6]^{2+} + nH_2O \rightarrow [Mg(OH)_n(H_2O)_{6-n}]^{2-n} + nH_3O^+ \quad (1)$$

In this manner, specific solvation is partially considered since one or two water molecules are present in the second coordination sphere. Deprotonation of Mg^{2+} can occur to a significant extent only if the free energy is negative. This is the case for a single external base (H_2O) assisted proton abstraction in $[Mg(H_2O)_6]^{2+}$ which is slightly but clearly exothermic (−4 kcal/mol) if the pentacoordinate metallohydroxide formed (**1b**) is allowed to retain a water molecule in its second coordination sphere. The energy requirement for a second water-assisted deprotonation is quite high (+65 kcal/mol) and continually rises with each additional proton abstraction, and we conclude that sequential deprotonations are probably relevant only for high energetical gas phase reactions of isolated species.

In eq 2, only the first shell ligands were included in the equilibrium. All waters that had migrated to the second sphere were treated as separate entities. Equation 2 confirms

$$[Mg(H_2O)_6]^{2+} + nH_2O \rightarrow [Mg(OH)_n(H_2O)_{6-n-x}]^{2-n} + nH_3O^+ + xH_2O \quad (2)$$

that a single deprotonation is astonishingly facile in the gas phase ($\Delta G \approx 1$ kcal/mol). This is clearly due to entropy effects (the number of free particles increases due to the reduction in the coordination number of magnesium which shifts the equilibrium to the right). The reaction enthalpy (ΔH) is endothermic (+12 kcal/mol), which indicates that an unsolvated pentacoordinate species (**1b′**) is intrinsically not as stable as $[Mg(H_2O)_6]^{2+}$. This stresses the need to explicitly consider specific solvation, especially in the active site of enzymes where individual solvent molecules are present but, due to the hydrophobic pocket, the properties of bulk water are not.

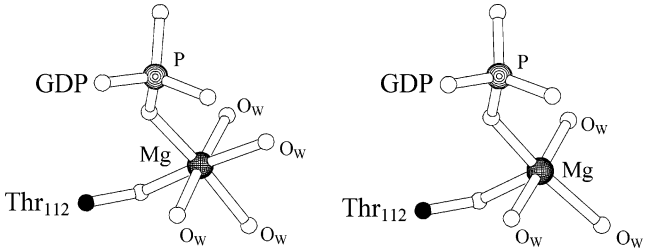

FIGURE 2: The two conformations of the magnesium ion in the Mg^{2+}−GDP complex of SRP GTPase Ffh (O_w = water ligand) as reported in ref *25* (pdb 1087).

Table 2: Selected NBO Properties of $[Mg(H_2O)_6]^{2+}$ and **1b′** [a]

	electronic configuration	atomic charge		bond index	
$Mg(H_2O)_6]^{2+}$	[core]3s(0.19)3d(0.01)	Mg	+1.792	Mg−O	0.063
		O	−1.013		
1b′ [b]	[core]3s(0.16)3d(0.01)	Mg	+1.825	Mg−O_{OH}	0.077
		O_{OH}	−1.383	Mg−O_{ax}	0.064
		O_{ax}	−1.002	Mg−O_{eq}[c]	0.061
		O_{eq}[c]	−1.032		

[a] Calculated at the B3LYP/aug-cc-pVTZ level of theory. [b] Pentacoordinate with only five ligands present. [c] Average value.

Comparison of both equilibrium positions in Table 1 indicates that solvation by one water molecule affects both ΔG (5 kcal/mol stabilization) and ΔH (one water in the second coordination sphere provides ca. 16 kcal/mol of enthalpic stabilization energy). We are now investigating specific as well as bulk solvation of these hydroxide species in more detail (increasing the number of waters in the second solvation sphere and/or placing the species of interest in a dielectric field to model bulk solvation) and will report our results in a forthcoming paper. In our opinion, this behavior of magnesium should be extremely relevant for understanding its mode of action in enzyme pockets.

Quite recently, an X-ray analysis (2.1 Å resolution) of the Mg^{2+}−GDP complex of the SRP GTPase Ffh has reported that SRP GTPase can assume two different conformations (*25*). In the solid-state structures of these conformers, the position of the bound Mg^{2+} ion and its coordinating waters could be quite well resolved. One conformer contains magnesium bound in a characteristic hexacoordinated Mg^{2+}−GDP binding domain very similar to those found in other members (*26*, *27*) of the GTPase superfamily (Figure 2) (*25*). The second conformer exhibits an "unusual" (*25*) pentacoordinated Mg^{2+} which, in light of the calculations presented here, we suggest is most likely a hydroxide species and that either the hydroxyl group of Thr112 or a water ligand has been deprotonated under the crystallization conditions. We furthermore suggest that such a conformational equilibrium could possibly have implications for the gating mechanism of GTPases.

Extensive NBO analyses of the binding situation in $[Mg(H_2O)_6]^{2+}$ and **1b′** reveal that the binding interactions, regardless of the coordination geometry, are, as expected, predominantly electrostatic in nature (Table 2). There is a significant charge transfer from the ligands to magnesium (originating from the sp-hybridized lone pair orbital on oxygen that points toward the central ion). This transferred charge resides primarily in the 3s orbital. A detailed analysis of the NBO data did not reveal concrete reasons for why

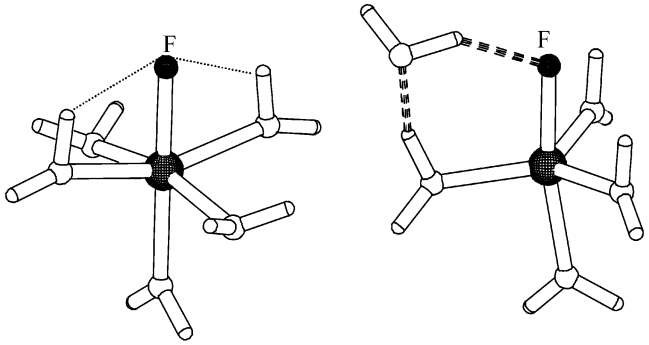

FIGURE 3: Ball and stick diagrams of selected conformations of the $[MgF(OH_2)_5]^+$ ion. Structure **2a** is a transition structure for the migration of an equatorial water into the second coordination sphere. Structure **2b** is the most stable pentacoordinated minimum found on the hypersurface. Calculated at the B3LYP/aug-cc-pVTZ level of theory.

deprotonation stabilizes the pentacoordinate geometry. We suspect that small, multireference components involving the d orbitals on magnesium are involved in helping to determine the preferred coordination geometry. We are currently attempting to perform multireference calculations on **1b′** to further investigate the electronic reasons for a coordination change upon deprotonation.

Fluoride Ligand. Since fluoride ligands are isoelectronic with hydroxides, we then investigated the coordination behavior of $[MgF(H_2O)_5]^+$ (**2**). Completely analogous to the hydroxide complex, the hexacoordinated species **2a** (Figure 3) is a transition structure (with a very low lying negative frequency) for migration of a water into the second coordination sphere. The pentacoordinated geometry **2b** is 2.1 kcal/mol more stable than **2a** at the B3LYP/aug-cc-pVTZ level of theory.

Carboxylate Ligands. $[Mg(H_2O)_{6-n}(HCO_2)_n]^{2-n}$ species have been extensively studied by several research groups at varying levels of theory (all, however, explicitly assumed a coordination number of 6 and considered only up to a maximum of four carboxylates) (*10c,f,g*). Repeating these calculations and explicitly considering that the coordination number of magnesium could possibly vary led to the species illustrated in Figure 4. In complete accord with the previous studies (*10c,f,g*) and in direct contrast to the mixed OH^-/H_2O species **1** or the F^-/H_2O species **2**, no stable pentacoordinate species could be found for *any* combination of six H_2O/HCO_2^- ligands at the B3LYP/aug-cc-pVTZ level of theory. Hydrated magnesium complexes containing carboxylate rests clearly prefer an octahedral coordination geometry. Species **3a′** ($[Mg(H_2O)_4(HCO_2)]^+$; not illustrated) in which we had removed one water molecule and explicitly constrained the HCO_2^- ligand to bind in a monodentate manner was the only species for which we succeeded in locating a trigonal bipyramidal local minimum. However, this structure is not stable toward specific solvation. As soon as a single water molecule was reintroduced anywhere in the second sphere and the structure reoptimized, the magnesium ion spontaneously incorporated this sixth ligand (water) into its first coordination sphere.

In contrast to hydroxide ligands with a localized negative charge, mesomeric delocalization in HCO_2^- allows the

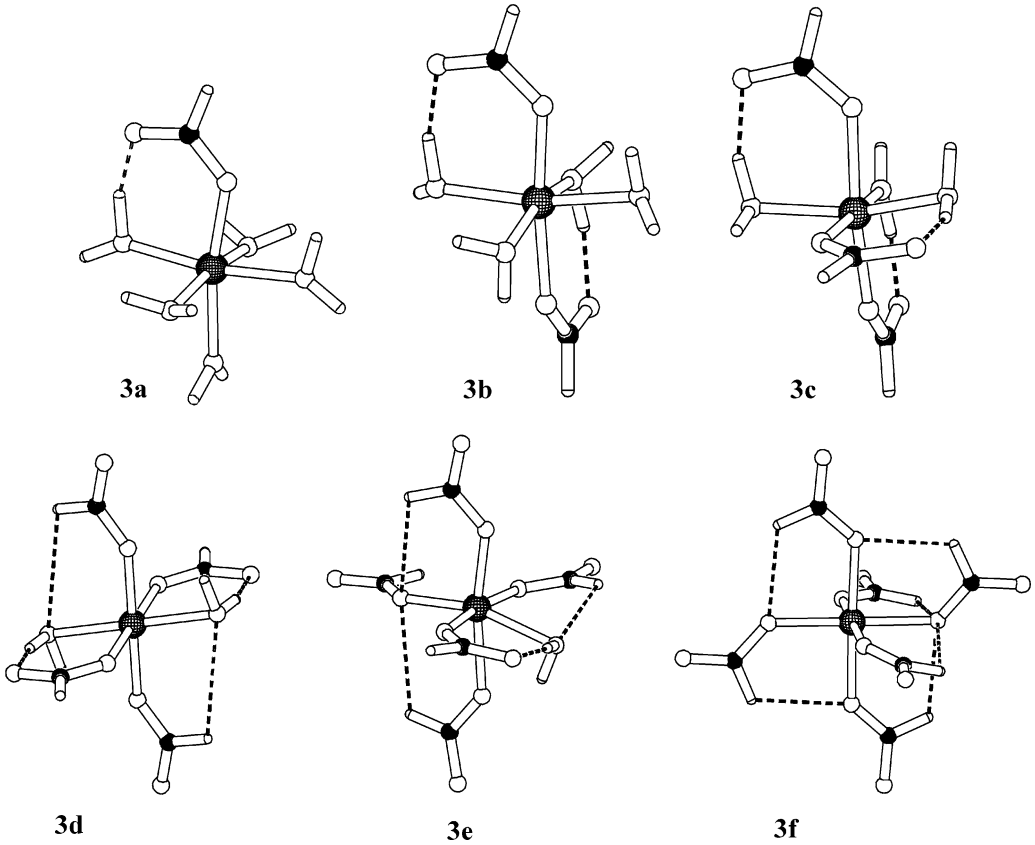

FIGURE 4: Ball and stick diagrams of the most stable conformation of $[Mg(H_2O)_{6-n}(HCO_2)_n]^{2-n}$ ions ($n = 0 \rightarrow 6$). B3LYP/aug-cc-pVTZ results except for **3f**, which was optimized at the B3LYP/lanl2dz level of theory.

Table 3: Thermodynamical Parameters (kcal/mol) for Carboxylate (HCO_2^-) Exchange in $[Mg(H_2O)_6]^{2+}$ Ions as Well as Deprotonation Equilibria for Mixed $[Mg(H_2O)_{6-n}(HCO_2)_n]^{2+}$ Species[a]

n	ΔG	ΔH	$T\Delta S$
	$[Mg(H_2O)_6]^{2+} + nHCO_2^- \rightarrow$ $[Mg(H_2O)_{6-n}(HCO_2)_n]^{2-n} + nH_2O$		
1	−199.3	−199.8	−0.5
2	−316.3	−320.2	−3.6
3	−352.3	−358.0	−5.2
4	−306.1	−310.0	−3.6
5	−212.1	−212.6	−0.5
6[b]	−23.1	−25.1	−1.8
	$[Mg(H_2O)_{6-n}(HCO_2)_n]^{2-n} + H_2O \rightarrow$ $[Mg(OH)(H_2O)_{5-n}(HCO_2)_n]^{1-n} + H_3O^+$		
1[b,c]	73.9	72.7	−1.1
2[b,c]	155.8	155.0	−0.1
3[b,c]	241.5	244.4	2.6
4[b,c]	305.6	309.1	3.1

[a] Calculated at the B3LYP/aug-cc-pVTZ level of theory. [b] B3LYP/aug-cc-pVTZ//B3LYP/lanl2dz energies. [c] A total of six ligands are present; in each case a ligand spontaneously left the first coordination sphere to yield a pentacoordinated central ion (Figure 5).

exchange of all six waters although exchange of the sixth ligand is barely exothermic in the gas phase (Table 3). Wherever possible, this charge delocalization is supported via strong hydrogen bonds to neighboring waters or ($n > 3$) carboxylate ligands. The thermodynamic equilibrium exchange data calculated here (Table 3) quite satisfactorily match those reported in earlier studies (*9c,f,g*). In the gas phase, exchange is thermodynamically favored (large negative ΔG due to strong Coulomb interactions) until a maximum of three carboxylates has been reached. We recommend the cited literature (*9c,f,g*) for an extensive discussion of this topic (especially the influence of the solvent on the equilibrium position).

We went on to deprotonate a water molecule in each of the species illustrated in Figure 4. Due to the large size of these mixed ligand complexes as well as the large number of possible conformations, it proved necessary to optimize these complexes at the somewhat lower (B3LYP/lanl2dz) computational level. The presence of a hydroxide ligand again resulted in a spontaneous lowering of the coordination nimber to generate trigonal bipyramidal complexes in which one of the ligands had migrated to the second coordination sphere. The most stable conformation found for each complex (several quasi-isoenergetical minima exist for each possibility) is illustrated in Figure 5.

When one or two carboxylates are present (**4a** and **4b**), a water is preferentially excluded from the first coordination sphere. For the case $n = 3$ (**4c**), a carboxylate is preferably lost, probably because the magnesium is not capable of stabilizing the additional negative charge in the gas phase without an extensive network of hydrogen bond stabilization (which is present for $n = 4$; **4d**).

Deprotonation of a water molecule in **3a** has been studied at the HF/6-31G* [and partially at the MP2(fc)/6-31+G*] level of theory (*10g*). Although no symmetry was imposed during optimizations, the authors did not report finding pentacoordinate intermediates (*10g*). In the course of our studies, we found that the HF level of theory is not capable of reliably yielding energetically stable pentacoordinate species. In view of the documented experimental findings of such species (*13*, *25*) which we discuss in the course of

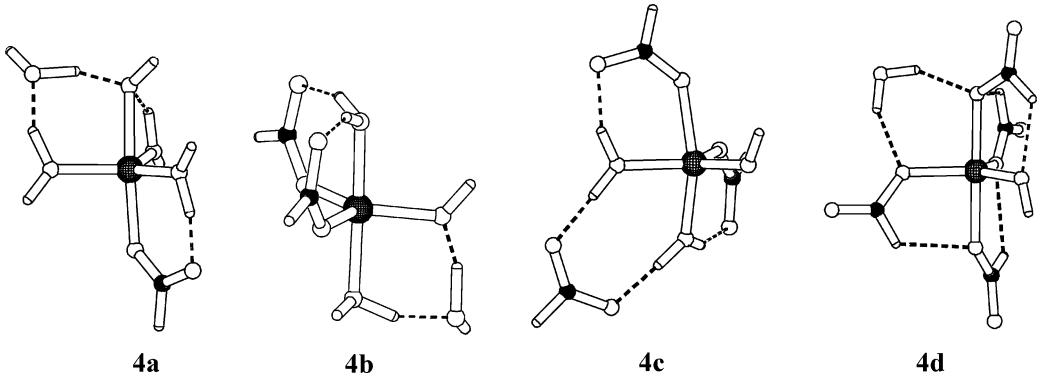

FIGURE 5: Ball and stick diagrams of the most stable conformation found for $[Mg(OH)(H_2O)_{5-n}(HCO_2)_n]^{1-n}$ ions ($n = 0 \rightarrow 4$). Optimized at the B3LYP/lanl2dz level of theory.

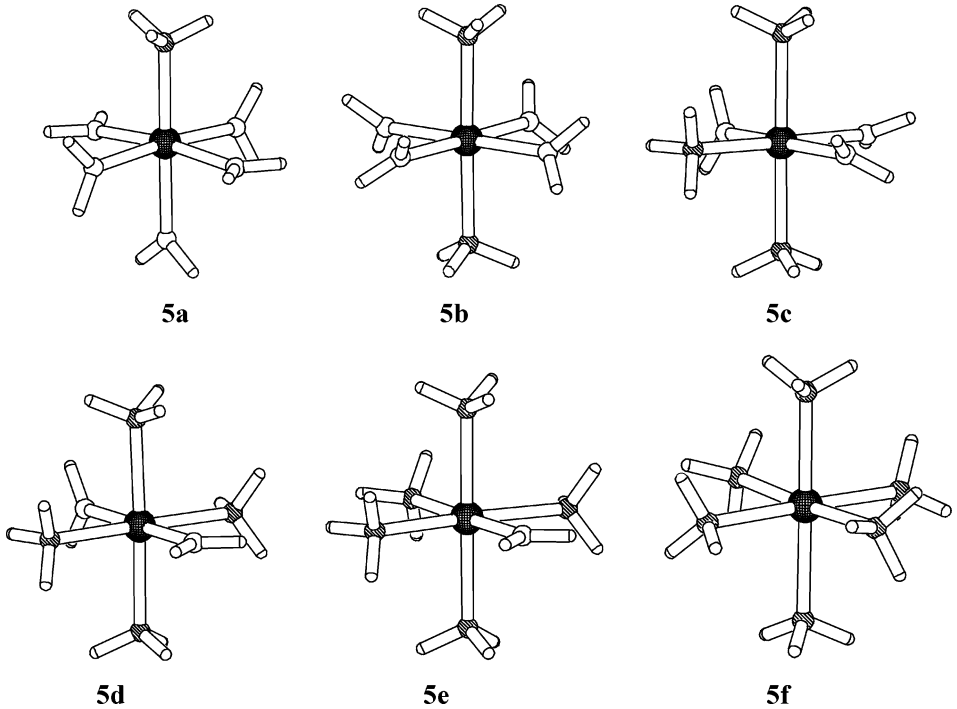

FIGURE 6: Ball and stick diagrams of the most stable conformation of $[Mg(NH_3)_n(OH_2)_{6-n}]^{2+}$ ions ($n = 1 \rightarrow 6$). Calculated at the B3LYP/aug-cc-pVTZ level of theory.

Table 4: Thermodynamical Parameters (kcal/mol) for Ammonia Exchange in $[Mg(H_2O)_6]^{2+}$ [a]

n	ΔG	ΔH	$T\Delta S$
$[Mg(H_2O)_6]^{2+} + n NH_3 \rightarrow [Mg(H_2O)_{6-n}(NH_3)_n]^{2+} + n H_2O$			
1	−3.7	−2.7	0.9
2	−6.3	−4.9	1.2
3	−9.2	−7.8	1.3
4	−11.6	−11.0	0.5
5	−15.2	−13.6	1.5
6	−17.5	−16.1	1.3

[a] Calculated at the B3LYP/aug-cc-pVTZ level of theory.

this paper, we do not recommend the HF method for further work on such systems.

Proton transfer between two isolated waters in the gas phase is well-known to be extremely endothermic (*10g*). The presence of a magnesium ion completely eradicates this endothermicity, thus making proton transfers between an external water and $[Mg(H_2O)_6]^{2+}$ quite feasible, at least in the gas phase (Table 4; see also ref *10g*). Substitution of a water ligand for a carboxylate increases the energy required for proton transfer by ca. 78 kcal/mol, thus effectively blocking a proton transfer in the gas phase. We expect that solvent effects will considerably lower this value and are currently studying the effect of both specific and bulk solvation upon the equilibrium position.

Ammonia (Model for Lys/His). A statistical evaluation of biologically relevant crystal structures contained in the Cambridge structural database showed that Mg^{2+} generally binds six ligands (75% of the total number of structures found), and oxygen is the most likely ligand (77%) followed by nitrogen (16%) (*10d*). Harding has also performed statistical evaluations of the metal coordination sites in metalloproteins with much the same results (*28*). Interestingly enough, at lower coordination numbers (3, 4, and 5) the binding preference for nitrogen increases and even surpasses that for oxygen (*10d*). Chelating nitrogen atoms in amino acid chains that are capable of directly coordinating with Mg^{2+} are the amino group found in Lys or the imidazole nitrogens in His followed by the formamide unit in Asn and Glu side chains as well as the backbone amide group in protein chains. These latter groups are less commonly directly coordinated to Mg^{2+}; they are generally found in the second

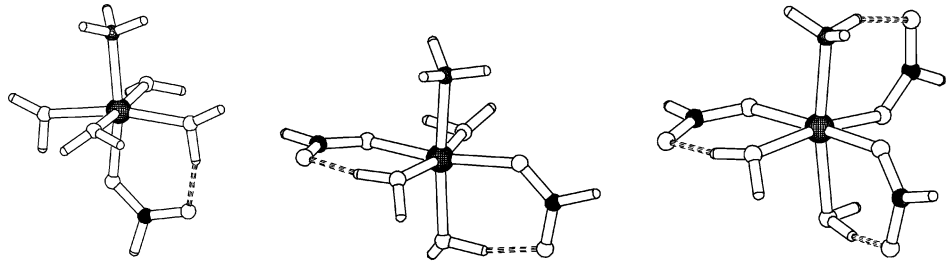

7a **7b** **7c**

FIGURE 7: Ball and stick diagrams of the most stable conformation of $[Mg(NH_3)(HCO_2)_n(OH_2)_{5-n}]^{1-n}$ ions ($n = 1 \rightarrow 3$). Calculated at the B3LYP/aug-cc-pVTZ level of theory.

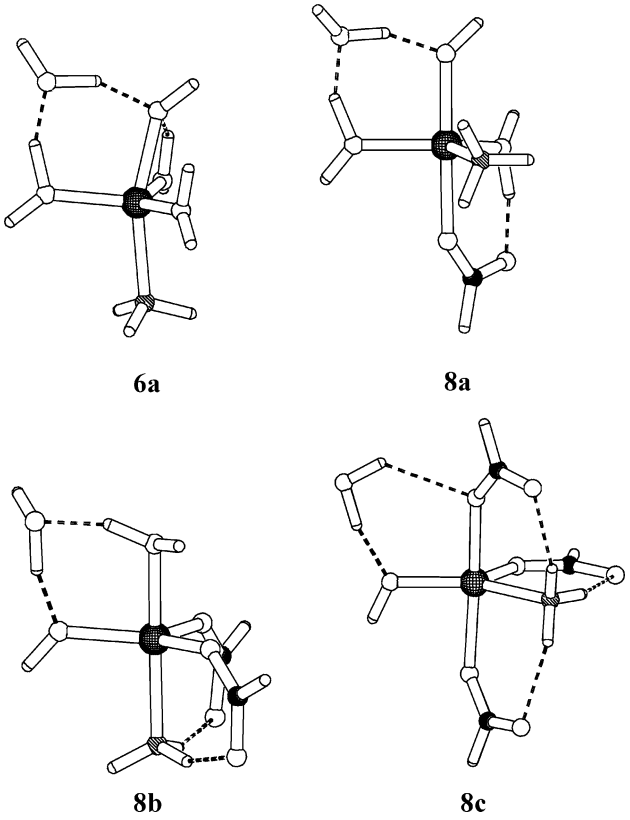

6a **8a**

8b **8c**

FIGURE 8: Ball and stick diagrams of the most stable conformation of $[Mg(OH)(NH_3)(HCO_2)_n(OH_2)_{4-n}]^{1-n}$ ions ($n = 0 \rightarrow 3$). Calculated at the B3LYP/lanl2dz level of theory.

coordination sphere or the oxygen in the amide bond is coordinated to Mg^{2+} instead of the nitrogen. We therefore chose to model nitrogen coordination in this study with NH_3, which is representative for Lys and can be extended to His bonding (*29*).

Analogous to its behavior with water ligands, magnesium shows a clear preference for coordination number 6 when it is bound to ammonia in $[Mg(NH_3)_6]^{2+}$ (Figure 6). All mixed $[Mg(H_2O)_{6-n}(NH_3)_n]^{2+}$ species **5** exhibit, as one would expect, energetically stable, hexacoordinated structures. Ammonia is a slightly worse ligand than water; the exchange equilibrium is weakly endothermic for each successive replacement of water. The free energies of ligand exchange are approximately additive (Table 4). Forcing the central Mg^{2+} to be pentacoordinated by providing it with only five ligands leads to energetically stable species in the gas phase. However, such pentavalent complexes are instable toward specific solvation. If a sixth ligand (either water or NH_3; it does not matter which) is placed in the second coordination sphere of a $[Mg(H_2O)_{5-n}(NH_3)_n]^{2+}$ species and allowed to freely optimize, the magnesium ion always pulls it into the first coordination sphere.

Table 5: Thermodynamic Parameters (kcal/mol) for Carboxylate (HCO_2^-) Exchange in $[Mg(NH_3)(H_2O)_6]^{2+}$ Ions as Well as Deprotonation Equilibria for Mixed $[Mg(NH_3)(H_2O)_{5-n}(HCO_2)_n]^{2+}$ Species[a]

n	ΔG	ΔH	$T\Delta S$
	$[Mg(NH_3)(H_2O)_5]^{2+} + nHCO_2^- \rightarrow$ $[Mg(NH_3)(H_2O)_{5-n}(HCO_2)_n]^{2-n} + nH_2O$		
1	−199.2	−199.8	−0.6
2	−314.6	−318.3	−3.7
3	−345.6	−351.5	−5.3
4	−297.5	−301.5	−3.7
	$[Mg(NH_3)(H_2O)_{5-n}(HCO_2)_n]^{2-n} + H_2O \rightarrow$ $[Mg(NH_3)(OH)(H_2O)_{4-n}(HCO_2)_n]^{1-n} + H_3O^+$		
1[b]	75.2	73.1	−1.9
2[b]	162.5	162.6	0.1
3[b]	244.6	246.6	1.9

[a] Calculated at the B3LYP/aug-cc-pVTZ level of theory. [b] B3LYP/aug-cc-pVTZ//B3LYP/lanl2dz energies. A total of six ligands are present; in each case a ligand spontaneously left the first coordination sphere to yield a pentacoordinated central ion (Figure 8).

Due to limited computational resources, we studied only the deprotonation of $[Mg(H_2O)_5NH_3)]^{2+}$, **5a**. Completely analogous to **1a**, removal of a proton from water and reoptimization led to a reduction in the coordination number at the central ion (complex **6a**, illustrated in Figure 8). Water and ammonia possess similar ligating properties, and it is not surprising that Gibb's free energy of the deprotonation equilibrium (**5a** + $H_2O \rightarrow$ **6a** + H_3O^+) is with −5.8 kcal/mol slightly exothermic. We predict that deprotonation of a water in the other mixed ligand complexes (**5b**−**e**) will also result in pentacoordinated species.

Biologically Relevant Mixed Ligand Systems. Magnesium-based enzymes often contain several (one to three) monodentately bound carboxylates (Asp/Glu) and (occasionally) one nitrogen (Lys/His) in the first coordination sphere of the metal cation (*10d*). We therefore considered the situation where one ammonia is present and a varying number of carboxylates and waters complete the first coordination sphere of Mg^{2+}. Although we could not explicitly consider all possible permutations, we managed to investigate the hypersurface throughly enough to be quite positive that the central ion prefers a octahedral coordination geometry for any combination of these ligands (the most stable conformers we found on the hypersurface are illustrated in Figure 7). No stable pentacoordinate species could be found on a

hypersurface containing one Mg^{2+} and a total of six ligands. A sixth ligand placed in the second coordination sphere of a pentavalent start geometry was always pulled in toward the Mg^{2+} upon free optimization. The calculated thermodynamic equilibrium exchange positions (Table 5) are quite similar to the H_2O/carboxylate case. Exchange is again favored until a maximum of three carboxylates is reached. Deprotonation of a Mg^{2+}-bound water ligand in complexes **7a**−**c** led to a spontaneous reduction in the coordination number, regardless of the number of carboxylates present (Figure 8).

CONCLUSION

Our computational findings, together with the solid state structures recently published for the Mg^{2+} complex of the SRP GTPase Ffh (*25*), present the very real possibility that a magnesium ion bound to an active site pocket in a metalloenzyme can, like the more flexible zinc ion, exhibit a differential coordination behavior in its mode of action. A necessary prerequisite for this seems to be the presence of a magnesium-bound hydroxide or fluoride, ligands which induce a pentavalent coordination geometry. This could be of quite some significance in the mode of action of Mg^{2+}-based enzymes, especially hydrolases, in which a metal-bound hydroxide is often postulated to be the active nucleophilic species. Water, carboxylate ligands, and ammonia are not capable of changing the preference of Mg^{2+} ions for octahedral coordination geometries.

ACKNOWLEDGMENT

We dedicate this article to our friend and colleague Dirk Walther on the occasion of his 65th birthday and use this opportunity to thank him for his many thoughtful insights on the subject of coordination chemistry. Furthermore, special thanks go to Ernst Anders and his research group for simulating discussions and valuable collaborations.

REFERENCES

1. Cowan, J. A., Ed. (1995) in *Biological Chemistry of Magnesium*, VCH, New York.
2. Ebel, H., and Gunther, T. (1980) Magnesium Metabolism−A Review, *J. Clin. Chem. Clin. Biochem. 18*, 257−270.
3. Black, C. B., Huang, H.-W., and Cowan, J. A. (1994) Biological Coordination Chemistry of Magnesium, Sodium and Potassium Ions. Protein and Nucleotide Binding Sites, *Coord. Chem. Rev. 135/136*, 165−202.
4. Dudev, T., and Lim, C. (2003) Principles Governing Mg, Ca and Zn Binding and Selectivity in Proteins, *Chem. Rev. 103*, 773−787.
5. Cowan, J. A. (1998) Magnesium Activation of Nuclease Enzymes−The Importance of Water, *Inorg. Chim. Acta 275/276*, 24−27.
6. (a) Barran, P. E., Walker, N. R., and Stace, A. J. (2000) Competitive Charge-Transfer Reactions in Small $[Mg(H_2O)_N]^{2+}$ Clusters, *J. Chem. Phys. 112*, 6173−6177; (b) Peschke, M., Blades, A. T., and Kebarle, P. J. (1998) Hydration Energies and Entropies for Mg^{2+}, Ca^{2+}, Sr^{2+}, and Ba^{2+} from Gas-Phase Ion−Water Molecule Equilibria Determinations, *J. Phys. Chem. A 102*, 9978−9985; (c) Ohtaki, H., and Radnai, T. (1993) Structure and Dynamics of Hydrated Ions, *Chem. Rev. 93*, 1157−1204; (d) Blades, A. T., Jayaweera, P., Ikonomou, M. G., and Kebarle, P. (1990) Studies of Alkaline Earth and Transition Metal M^{2+} Gas-Phase Ion Chemistry, *J. Chem. Phys. 92*, 5900−5906; (e) Caminiti, R., Licheri, G., Piccaluga, G., and Pinna, G. (1979) Diffraction of X-rays and Hydration Phenomena in Aqueous Solutions of $Mg(NO_3)_2$, *Chem. Phys. Lett. 61*, 45−49; (f) Albright, J. N. (1972) X-Ray Diffraction Studies of Aqueous Alkaline-Earth Chloride Solutions, *J. Chem. Phys. 56*, 3783−3786; (g) Neely, J., and Connick, R. (1970) Rate of Water Exchange from Hydrated Magnesium Ion, *J. Am. Chem. Soc. 92*, 3476−3478; (h) Matwiyoff, N. A., and Taube, H. (1968) Direct Determination of the Solvation Number of the Magnesium (II) Ion in Water, Aqueous Acetone, and Methanolic Acetone Solutions, *J. Am. Chem. Soc. 90*, 2796−2800; (i) see also literature contained therein.
7. (a) Markham, G. D., Glusker, J. P., and Bock, C. W. (2002) The Arrangement of First- and Second-Sphere Water Molecules in Divalent Magnesium Complexes: Results from Molecular Orbital and Density Functional Theory and from Structural Crystallography, *J. Phys. Chem. B 106*, 5118−5134; (b) Pye, C. C., and Rudolph, W. W. (1998) An ab Initio and Raman Investigation of Magnesium(II) Hydration, *J. Phys. Chem. A 102*, 9933−9943; (c) Bock, C. W., Kaufman, A., and Glusker, J. P. (1994) Coordination of Water to Magnesium Cations, *Inorg. Chem. 33*, 419−427; (d) see also literature contained therein.
8. (a) Martínez, J. M., Pappalardo, R. R., and Marcos, E. S. (1999) First-Principles Ion−Water Interaction Potentials for Highly Charged Monatomic Cations. Computer Simulations of Al^{3+}, Mg^{2+}, and Be^{2+} in Water, *J. Am. Chem. Soc. 121*, 3175−3184; (b) Trachtman, M., Markham, G. D., Glusker, J. P., George, P., and Bock, C. W. (1998) Interactions of Metal Ions with Water: Ab Initio Molecular Orbital Studies of Structure Bonding Enthalpies, Vibrational Frequencies and Charge Distributions. 1. Monohydrates, *Inorg. Chem. 37*, 4421−4431; (c) Pavlov, M., Siegbahn, P. E. M., and Sandström, M. (1998) Hydration of Beryllium, Magnesium, Calcium, and Zinc Ions Using Density Functional Theory, *J. Phys. Chem. A 102*, 219−228; (d) Katz, A. K., Glusker, J. P., Beebe, S. A., and Bock, C. W. (1996) Calcium Ion Coordination: A Comparison with That of Beryllium, Magnesium, and Zinc, *J. Am. Chem. Soc. 118*, 5752−5763; (e) Glendening, E. D., and Feller, D. (1996) Dication−Water Interactions: $M^{2+}(H_2O)_n$ Clusters for Alkaline Earth Metals M = Mg, Ca, Sr, Ba, and Ra, *J. Phys. Chem. 100*, 4790−4797; (f) Markham, G. D., Glusker, J. P., Bock, C. L., Trachtman, M., and Bock, C. W. (1996) Hydration Energies of Divalent Beryllium and Magnesium Ions: An ab Initio Molecular Orbital Study, *J. Phys. Chem. 100*, 3488−3497; (g) Bock, C. W., Katz, A. K., and Glusker, J. P. (1995) Hydration of Zinc Ions: A Comparison with Magnesium and Beryllium Ions, *J. Am. Chem. Soc. 117*, 3754−3765; (h) Kaupp, M., and Schleyer, P. v. R. (1992) Do Low-Coordinated Group 1−3 Cations $M^{n+}L_m$ (M^{n+} = K^+, Rb^+, Cs^+, Ca^{2+}, Sr^{2+}, Ba^{2+}, Sc^{3+}, Y^{3+}, La^{3+}; L = NH_3, H_2O, HF; m = 1−3) with a Formal Noble-Gas Electron Configuration Favor Regular or "Abnormal" Shapes?, *J. Phys. Chem. 96*, 7316−7323; (i) Bauschlicher, C. W., Jr., Sodupe, M., and Partridge, H. (1992) A Theoretical Study of the Positive and Dipositive Ions of $M(NH_3)_n$ and $M(H_2O)n$ for M = Mg, Ca, or Sr, *J. Chem. Phys. 96*, 4453−4463; (j) Marcos, E. S., Pappalardo, R. R., and Rinaldi, D. (1991) Effects of the Solvent Reaction Field on the Geometrical Structures of Hexahydrate Metallic Cations, *J. Phys. Chem. 95*, 8928−8932; (k) see also literature contained therein.
9. See for instance, the Cambridge Structural Database (CSD) at www.ccdc.cam.ac.uk.
10. (a) Dudev, T., Lin, Y., Dudev, M., and Lim, C. (2003) First-Second Shell Interactions in Metal Binding Sites in Proteins: A PDB Survey and DFT/CDM calculations, *J. Am. Chem. Soc. 125*, 3168−3180; (b) Dudev, T., and Lim, C. (2001) Metal Selectivity in Metalloproteins: Zn^{2+} vs Mg^{2+}, *J. Phys. Chem. B 105*, 4446−4452; (c) Dudev, T., and Lim, C. (2000) Metal Binding in Proteins: The Effect of the Dielectric Medium, *J. Phys. Chem. B 104*, 3692−3694; (d) Bock, C. W., Katz, A. K., Markham, G. D., and Glusker, J. P. (1999) Manganese as a Replacement for Magnesium and Zinc: Functional Comparison of the Divalent Ions, *J. Am. Chem. Soc. 121*, 7360−7372; (e) Dudev, T., Cowan, J. A., and Lim, C. (1999) Competitive Binding in Magnesium Coordination Chemistry: Water versus Ligands of Biological Interest, *J. Am. Chem. Soc. 121*, 7665−7673; (f) Dudev, T., and Lim, C. (1999) Incremental Binding Free Energies in Mg^{2+} Complexes: A DFT Study, *J. Phys. Chem. A 103*, 8093−8100; (g) Katz, A. K., Glusker, J. P., Markham, G. D., and Bock, C. W. (1998) Deprotonation of Water in the Presence of Carboxylate and Magnesium Ions, *J. Phys. Chem. B 102*, 6342−6350; (h) Garmer, D. R., and Gresh, N. (1994) A Comprehensive Energy Component Analysis of the Interaction of Hard and Soft Dications with Biological Ligands, *J. Am. Chem. Soc. 116*, 3556−3567; (i) Krauss, M., and Stevens, W. (1990) Analysis of Protein Metal Binding Selectivity in a Cluster Model, *J. Am. Chem. Soc. 112*, 1460−1466.

11. Markies, P. R., Akkerman, O. S., Bickelhaupt, F., Smeets, W. J. J., and Spek, A. L. (1991) X-Ray Structural Analyses of Organomagnesium Compounds, *Adv. Organomet. Chem. 32*, 147−226.
12. Walker, N., Dobson, M. P., Wright, R. R., Barran, P. E., Murrell, J. N., and Stace, A. J. (2000) A Gas-Phase Study of the Coordination of Mg^{2+} with Oxygen- and Nitrogen-Containing Ligands, *J. Am. Chem. Soc. 122*, 11138−11145.
13. (a) Rodriguez-Cruz, S. E., Jockusch, R. A., and Williams, E. R. (1999) Binding Energies of Hexahydrated Alkaline Earth Metal Ions, $M^{2+}(H_2O)_6$, M = Mg, Ca, Sr, Ba: Evidence of Isomeric Structures for Magnesium, *J. Am. Chem. Soc. 121*, 1986−1987; (b) Rodriguez-Cruz, S. E., Jockusch, R. A., and Williams, E. R. (1999) Hydration Energies and Structures of Alkaline Earth Metal Ions, $M^{2+}(H_2O)_n$, $n = 5-7$, M = Mg, Ca, Sr, and Ba, *J. Am. Chem. Soc. 121*, 8898−8906.
14. Cowan, J. A. (1998) Metal Activation of Enzymes in Nucleic Acid Biochemistry, *Chem. Rev. 98*, 1067−1087.
15. (a) Trachtman, M., Markham, G. D., Glusker, J. P., George, P., and Bock, C. W. (2001) Interactions of Metal Ions with Water: Ab Initio Molecular Orbital Studies of Structure, Vibrational Frequencies, Charge Distributions, Bonding Enthalpies, and Deprotonation Enthalpies. 2. Monohydroxides, *Inorg. Chem. 40*, 4230−4241; (b) Beyer, M., Williams, E. R., and Bondybey, V. E. (1999) Unimolecular Reactions of Dihydrated Alkaline Earth Metal Dications $M^{2+}(H_2O)_2$, M = Be, Mg, Ca, Sr, and Ba: Salt-Bridge Mechanism in the Proton-Transfer Reaction $M^{2+}(H_2O)_2 \rightarrow MOH^+ + H_3O^+$, *J. Am. Chem. Soc. 121*, 1565−1573; (c) Magnusson, E., and Moriarty, N. W. (1996) Binding Patterns in Single-Ligand Complexes of NH_3, H_2O, OH^-, and F^- with First Series Transition Metals, *Inorg. Chem. 35*, 5711−5719.
16. Sponer, J., Burda, J. V., Sabat, M., Leszczynski, J., and Hobza, P. (1998) Interaction between the Guanine-Cytosine Watson−Crick DNA Base Pair and Hydrated Group IIa (Mg^{2+}, Ca^{2+}, Sr^{2+}, Ba^{2+}) and Group IIb (Zn^{2+}, Cd^{2+}, Hg^{2+}) Metal Cations, *J. Phys. Chem. A 102*, 5951−5957.
17. Kluge, S. (2003) Entwicklung eines Modells für die Inositol Monophosphatase, Friedrich Schiller University, Jena, Germany; Diplomarbeit, Kluge, S., and Weston, J., work in progress.
18. (a) Becke, A. D. (1993) Density-functional thermochemistry. III. The Role of Exact Exchange, *J. Chem. Phys. 98*, 5648−5652; (b) Lee, C., Yang, W., and Parr, R. G. (1988) Development of the Colle-Salvetti Correlation-Energy Formula into a Functional of the Electron Density, *Phys. Rev. B 37*, 785−789.
19. Frisch, M. J., Trucks, G. W., Schlegel, H. B., Scuseria, G. E., Robb, M. A., Cheeseman, J. R., Zakrzewski, V. G., Montgomery, J. A., Stratmann, R. E., Burant, J. C., Dapprich, S., Millam, J. M., Daniels, A. D., Kudin, K. N., Strain, M. C., Farkas, O., Tomasi, J., Barone, V., Cossi, M., Cammi, R., Mennucci, B., Pomelli, C., Adamo, C., Clifford, S., Ochterski, J., Petersson, G. A., Ayala, P. Y., Cui, Q., Morokuma, K., Rega, N., Salvador, P., Dannenberg, J. J., Malick, D. K., Rabuck, A. D., Raghavachari, K., Foresman, J. B., Cioslowski, J., Ortiz, J. V., Baboul, A. G., Stefanov, B. B., Liu, G., Liashenko, A., Piskorz, P., Komaromi, I., Gomperts, R., Martin, R. L., Fox, D. J., Keith, T., Al-Laham, M. A., Peng, C. Y., Nanayakkara, A., Challacombe, M., Gill, P. M. W., Johnson, B., Chen, W., Wong, M. W., Andres, J. L., Gonzalez, C., Head-Gordon, M., Replogle, E. S., and Pople, J. A. (2002) *Gaussian 98, Revision A.11.4*, Gaussian Inc., Pittsburgh, PA.
20. Frisch, M. J., Trucks, G. W., Schlegel, H. B., Scuseria, G. E., Robb, M. A., Cheeseman, J. R., Montgomery, J. A., Jr., Vreven, T., Kudin, K. N., Burant, J. C., Millam, J. M., Iyengar, S. S., Tomasi, J., Barone, V., Mennucci, B., Cossi, M., Scalmani, G., Rega, N., Petersson, G. A., Nakatsuji, H., Hada, M., Ehara, M., Toyota, K., Fukuda, R., Hasegawa, J., Ishida, M., Nakajima, T., Honda, Y., Kitao, O., Nakai, H., Klene, M., Li, X., Knox, J. E., Hratchian, H. P., Cross, J. B., Adamo, C., Jaramillo, J., Gomperts, R., Stratmann, R. E., Yazyev, O., Austin, A. J., Cammi, R., Pomelli, C., Ochterski, J. W., Ayala, P. Y., Morokuma, K., Voth, G. A., Salvador, P., Dannenberg, J. J., Zakrzewski, V. G., Dapprich, S., Daniels, A. D., Strain, M. C., Farkas, O., Malick, D. K., Rabuck, A. D., Raghavachari, K., Foresman, J. B., Ortiz, J. V., Cui, Q., Baboul, A. G., Clifford, S., Cioslowski, J., Stefanov, B. B., Liu, G., Liashenko, A., Piskorz, P., Komaromi, I., Martin, R. L., Fox, D. J., Keith, T., Al-Laham, M. A., Peng, C. Y., Nanayakkara, A., Challacombe, M., Gill, P. M. W., Johnson, B., Chen, W., Wong, M. W., Gonzalez, C., and Pople, J. A. (2003) *Gaussian 03, Revision B.04*, Gaussian, Inc., Pittsburgh, PA.
21. (a) Davidson, E. R. (1996) Comment on Dunning's Correlation-Consistent Basis Sets, *Chem. Phys. Lett. 260*, 514−518; (b) Kendall, R. A., Dunning, T. H., Jr., and Harrison, R. J. (1992) Electron affinities of the first-row atoms revisited. Systematic basis sets and wave functions, *J. Chem. Phys. 96*, 6796−6806.
22. Dunning, T. H., Jr. (1989) Gaussian Basis Sets for Use in Correlated Molecular Calculations. I. The Atoms Boron through Neon and Hydrogen, *J. Chem. Phys. 90*, 1007−1023.
23. (a) Reed, A. E., Curtis, L. A., and Weinhold, F. (1988) Intermolecular interactions from a natural bond orbital, donor−acceptor viewpoint, *Chem. Rev. 88*, 899−926; (b) Reed, A. E., Weinstock, L. R. B., and Weinhold, F. (1985) Natural Population Analysis, *J. Chem. Phys. 83*, 735−746; (c) Reed, A. E., and Weinhold, F. (1983) Natural Bond Orbital Analysis of Near-Hartree−Fock Water Dimer, *J. Chem. Phys. 78*, 4066−4073.
24. Glendening, E. D., Badenhoop, J. K., Reed, A. E., Carpenter, J. E., Bohmann, J. A., Morales, C. M., and Weinhold, F. (2001) *NBO 5.0*, Theoretical Chemistry Institute, University of Wisconsin, Madison, WI, http://www.chem.wisc.edu/∼nbo5/.
25. Focia, P. J., Alam, H., Lu, T., Ramirez, U. D., and Freymann, D. M. (2004) Novel Protein and Mg^{2+} Configurations in the Mg^{2+}-GDP Complex of the SRP GTPase Ffh, *Proteins: Struct., Funct., Bioinform. 54*, 222−230.
26. (a) Padmanabhan, S., and Freymann, D. M. (2001) The Conformation of Bound GMPPPNP Suggests a Mechanism for Gating the Active Site of the SRP GTPase, *Structure 9*, 859−867; (b) Zhang, B., Zhang, Y., Wang, Z., and Zheng, Y. (2000) The Role of Mg^{2+} Cofactor in the Guanine Nucleotide Exchange and GTP Hydrolysis Reactions of Rho Family GTP-binding Proteins, *J. Biol. Chem. 275*, 25299−25307.
27. (a) Chen, Z., Wells, C. D., Sternweis, P. C., and Sprang, S. R. (2001) Structure of the rgRGS Domain of p115RhoGEF, *Nat. Struct. Biol. 8*, 805−809; (b) Coleman, D. E., and Sprang, S. R. (1999) Structure of $G_{i\alpha1}$. GppNHp, Autoinhibition in a G_α Protein−Substrate Complex, *J. Biol. Chem. 274*, 16669−16672; (c) Coleman, D. E., and Sprang, S. R. (1998) Crystal Structures of the G Protein $G_{i\alpha1}$ Complexed with GDP and Mg^{2+}: A Crystallographic Titration Experiment, *Biochemistry 37*, 14376−14385; (d) Sprang, S. R., and Coleman, D. E. (1998) Invasion of the Nucleotide Snatchers: Structural Insights into the Mechanism of G Protein GEFs, *Cell 95*, 155−158; (e) Sprang, S. R. (1997) G Proteins, Effectors and GAPs: Structure and Mechanism, *Curr. Opin. Struct. Biol. 7*, 849−856; (f) Sunahara, R. K., Tesmer, J. J. G., Gilman, A. G., and Sprang, S. R. (1997) Crystal Structure of the Adenylyl Cyclase Activator $G_{s\alpha}$, *Science 278*, 1943−1947; (g) Tesmer, J. J. G., Berman, D. M., Gilman, A. G., and Sprang, S. R. (1997) Structure of RGS4 Bound to AlF_4^--Activated $G_{i\alpha1}$: Stabilization of the Transition State for GTP Hydrolysis, *Cell 89*, 251−261; (h) Tesmer, J. J. G., Sunahara, R. K., Gilman, A. G., and Sprang, S. R. (1997) Crystal Structure of the Catalytic Domains of Adenylyl Cyclase in a Complex with $G_{s\alpha}$.GTPγS, *Science 278*, 1907−1915; (i) Sprang, S. R. (1997) G Protein Mechanisms: Insights from Structural Analysis, *Annu. Rev. Biochem. 66*, 639−678; (j) Coleman, D. E., Berghuis, A. M., Lee, E., Linder, M. E., Gilman, A. G., and Sprang, S. R. (1994) Structures of Active Conformations of G(I−Alpha-1) and the Mechanism of GTP Hydrolysis, *Science 265*, 1405−1412.
28. (a) Harding, M. M. (2004) The architecture of metal coordination groups in proteins, *Acta Crystallogr. D60*, 849−859; (b) Harding, M. M. (2001) Geometry of Metal−Ligand Interactions in Proteins, *Acta Crystallogr. D57*, 401−411; (c) Harding, M. M. (2000) The Geometry of Metal−Ligand Interactions Relevant to Proteins. Ii. Angles at the Metal Atom, Additional Weak Metal-Donor Interactions, *Acta Crystallogr. D56*, 857−867; (d) Harding, M. M. (1999) Geometry of Metal−Ligand Interactions Relevant to Proteins, *Acta Crystallogr. D55*, 1432−1443.
29. Mauksch, M., Bräuer, M., Weston, J., and Anders, E. (2001) New Insights into the Mechanistic Details of the Carbonic Anhydrase Cycle as Derived from the Model System $[NH_3)_3Zn(OH)]^+/CO_2$: How Does the H_2O/HCO_3^- Replacement Step Occur?, *ChemBioChem. 2*, 190−198.

BI047454J